Journal of the European Ceramic Society 20 (2000) 589–597

Effect of coating deposition temperature on monazite coated fiber

R.S. Hay[a,*], E. Boakye[b], M.D. Petry[b]

[a]*Air Force Research Laboratory, Materials Directorate, Wright Patterson Air Force Base, OH 45433, USA*
[b]*UES Inc., 4401 Dayton-Xenia Road, Dayton, OH 45432, USA*

Accepted 13 August 1999

Abstract

Monazite ($LaPO_4$) was continuously coated on 3M Nextel™ 720 fiber tows with an ethanolic precursor using hexadecane for immiscible liquid displacement. Coating deposition temperatures were varied from 900 to 1300°C. Fibers coated at 900°C were heat-treated up to 100 h at 1200°C. Coated fibers were characterized by analytical TEM, and tensile strengths were measured by single filament tensile tests. The monazite precursor was characterized by X-ray, DTA/TGA, and mass spectrometry. Microstructure evolution was complex and may have involved recrystallization of large defective grains into smaller grains and then subsequent growth of these grains, along with coarsening of porosity. After 100 h at 1200°C there was significant roughening of the coating–fiber interface, with facetting of alumina grains in the fiber and some lanthanum segregation to these facetted boundaries. Spheroidization of thin coatings was also observed. Tensile strength of coated fiber decreased with increasing deposition temperature and with time at temperature after deposition. Possible reasons for the strength decrease are discussed. Published by Elsevier Science Ltd.

Keywords: Aluminosilicate fibers; Coating; Grain growth; Interfaces; $LaPO_4$; Mechanical properties

1. Introduction

Improvement of intermediate and high temperature properties of ceramic matrix composites (CMCs) requires an oxidation resistant alternative to carbon or boron nitride fiber-matrix interfaces.[1–6] One possible alternative is monazite ($LaPO_4$). Monazite is refractory (mp 2072C) and thermochemically stable with many other common refractory oxides such as alumina and mullite.[7–9] Crack deflection and fiber pushout experiments, as well as some limited mechanical tests on composites suggest that monazite bonds weakly with other oxides.[8–10] Some similar results were found for xenotime (YPO_4)[11] and scheelite ($CaWO_4$).[12] Monazite containing ceramics were demonstrated to be machineable,[13] which implies significant plasticity from some combination of cleavage microcracking, twinning, or dislocation glide.[14]

Use of monazite as a fiber-matrix interface in CMCs requires that it either be coated on fibers or formed in situ between the fiber and matrix during processing. Sol and solution precursors have been used to coat fiber tows with monazite,[6] as has continuous chemical vapor deposition (CVD).[10,15,16] Limited experiments demonstrate crack deflection and fiber pullout in tensile tests of composites with CVD monazite coated fiber tows.[10] For liquid-phase precursors, crack deflection and debonding have only been demonstrated on composites with low volume fractions of dip coated, large diameter (100 μm) single crystal alumina (Saphikon®) monofilaments.[8] The thickness uniformity of sol and solution derived coatings on filaments in fiber tows is often poor, although stoichiometry is easily controlled.[6] In contrast, limited data suggest that CVD coatings have good thickness uniformity, but are sometimes off stoichiometry.[15,16]

Filament tensile strength is often degraded during fiber coating,[6,17–19] or during exposure to various environments.[20,21] Strength increases after coating or environmental exposure are also known.[22,23] Large differences in tensile strength have been observed between fibers coated with different monazite precursors.[6] Preliminary indications of a strong tensile strength dependence on coating temperature were also found. Excessive degradation in fiber tensile strength

* Corresponding author Tel.:1-937 255 9825; fax: 1 937 656 4296.
E-mail address: hayrs@ml.wl.wpafb.af.mil (R.S. Hay).

0955-2219/00/$ - see front matter. Published by Elsevier Science Ltd.
PII: S0955-2219(99)00257-5

may cause an otherwise functional coating to appear non-functional. Knowledge of the conditions under which degradation occurs is therefore important for interface evaluation, besides the obvious importance to composite strength and failure mechanisms.[24–26] Isolation of the causes of strength degradation may lead to improved coating methods that minimize this degradation.

This work describes characteristics of 3M Nextel 720 fiber coated with monazite between 900 and 1300°C. Characteristics of the 900°C coated fiber after heat-treatment for up to 100 h at 1200°C are also described. Changes in composition and microstructure of the coating and fiber were observed by TEM. Precursor and coating evolution were monitored by X-ray, TEM, and DTA/TGA. Precursor gas evolution was observed by DTA/TGA and mass spectrometry. Strength of coated and uncoated fibers were measured by single filament tensile tests. Changes in coating characteristics with temperature were compared with changes in the coated filament tensile strength. The results are analyzed and possible degradation mechanisms are discussed.

2. Experiments

Lanthanum nitrate and phosphorous pentoxide were dissolved in dry ethanol with the appropriate stoichiometry to form 50 g/l of monazite.[6] These solutions had a density of 0.84 g/cm^3 and a viscosity of 1.39 mPa·s, as measured in a Brookfield programmable rheometer (model DV-III) at a shear rate of 1/300. The precursor was characterized after a 1 h heat-treatment at 1200°C by X-ray diffraction in a Rigaku Rotaflex Diffractometer. Differential thermal analysis (DTA) and thermogravimetric analysis (TGA) were done in a Netzsch STA-409 at 10°C/min up to 1500°C after the precursor was dried for 1 h at 140°C. Mass spectrometry of gases evolved from the precursor was done in a Balzers QMS 420 at 5°C/min up to 1050°C. The measurement was done in argon so measurement overlap with atmospheric gases could be eliminated. A more detailed description of the mass spectrometry equipment is given elsewhere.[27]

3M Nextel 720 alumina–mullite fibers[28–30] were continuously coated with the monazite precursor in a vertical coater using hexadecane for immiscible liquid displacement. A coating speed of 1.4 cm/s in an air atmosphere was used for all experiments. The furnace hot zone was about 8 cm in length, and total furnace length was 30 cm. The fiber coating apparatus and procedures are described in more detail elsewhere.[6,31–34] The fibers were desized in air at 1000°C and 2.8 cm/s before coating. Coating runs were done at 900, 1000, 1100, 1200, and 1300°C. Some fibers coated at 900°C were then heat-treated at 1200°C for 0.2, 2, 10, or 100 h in a furnace with $MoSi_2$ heating elements.

TEM thin foils were made of coated fiber cross-sections as described elsewhere.[35,36] Thin foils were observed in either a JEOL 2000 FX operating at 200 kV, or in a Phillips CM 200 FEG operating at 200 kV. Energy dispersive spectroscopy (EDS) measurements were done in the Phillips CM 200 FEG with a 5 nm spot size and a windowless detector.

Coated filament tensile strengths and Weibull modulii were measured using a 2.54 cm gauge length with 75 tests. For controls, tensile strengths were also measured for filaments that had been heat-treated without coating, and for filaments that had been passed through the fiber coater under conditions that mimicked a coating run, but without coating deposition. Further details of tensile strength measurement are presented elsewhere.[37]

3. Results

3.1. X-ray, DTA/TGA, and mass spectrometry

Precursor heat-treated for 1 h at 1200°C has monazite X-ray peaks and small La_3PO_7 peaks, indicating a slight phosphate deficiency from the monazite stoichiometry (Fig. 1). A weak exotherm at about 450°C and a weak endotherm at about 950°C were the only significant DTA features (Fig. 2). About 4.5% of the precursor mass was lost between 100 and 550°C. Above 550°C mass loss was less rapid, but an additional 1.5% was still lost between 550 and 1500°C. This 1.5% loss corresponds to a volume of gas that is at least 10 to 50 times larger than the volume of monazite it evolved from. A slight increase in mass loss at around 950°C correlates with the temperature of the weak DTA endotherm. By mass spectrometry, only H_2O, N_2 or CO, and N_2O or CO_2 were observed to evolve in significant quantities above 600°C (Fig. 3). Lack of amu resolution precluded distinguishing N_2 from CO (amu 28) or N_2O from CO_2 (amu 44). Methane (CH_4) and CH_3 evolution at 500°C roughly corresponds to the

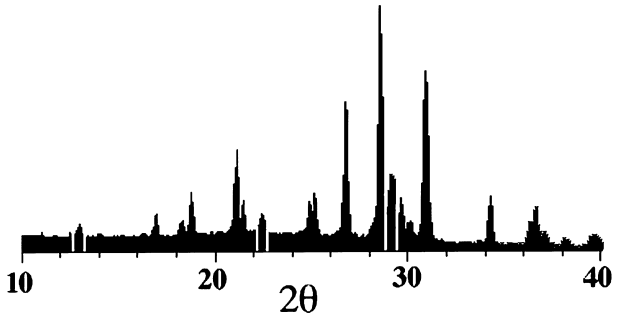

Fig. 1. X-ray diffraction pattern of monazite from precursor heat-treated for 1 h at 1200°C. All peaks correspond to monazite except those highlighted in gray, which correspond to La_3PO_7.

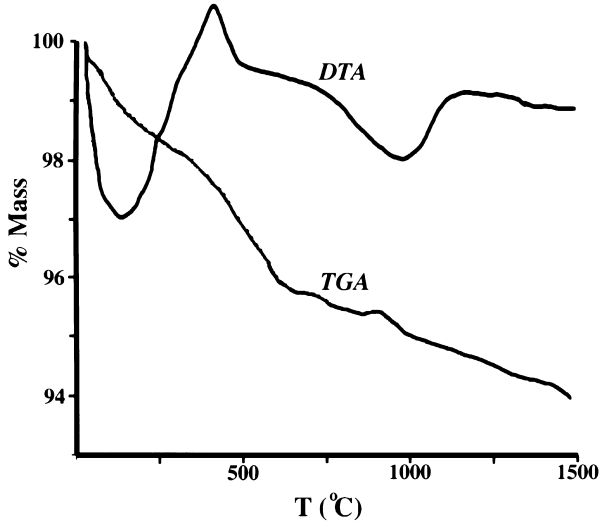

Fig. 2. DTA/TGA of monazite precursor. Scale for DTA trace is not given.

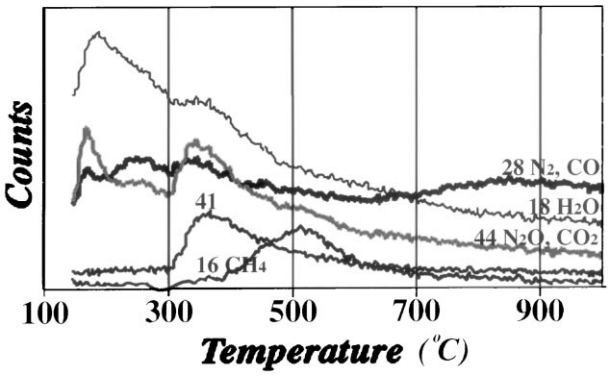

Fig. 3. Mass spectrometry of gas evolution from monazite precursor.

DTA exotherm at about 450°C. The mass spectrometry specimen was black after the measurement, suggesting incomplete oxidation of carbonaceous species in the argon environment.

3.2. Coatings — general

Coating thickness and morphology was similar to that observed previously for this precursor.[6] Coating coverage was continuous. Coating bridges between filaments, thin poorly crystallized coatings, and debonded or "buckled" coatings were occasionally observed (Fig. 4). Significant place to place variations in pore volume fraction and size were also observed. Coating thickness averaged about 80 nm, with variations between 30 and 120 common. Although a small amount of La_3PO_7 was observed by X-ray, no evidence of any phase other than monazite was found in fiber coatings by TEM.

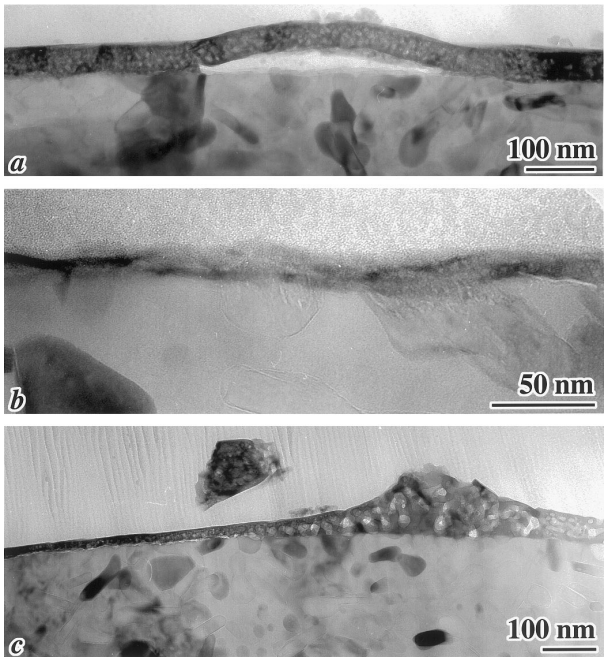

Fig. 4. TEM pictures of typical coating anomalies: (a) Debonded coating; (b) Thin, poorly crystallize coating; (c) Broken filament to filament coating bridge.

3.3. Coating temperature

The most obvious change in the coatings as deposition temperature increased from 900 to 1300°C was a decrease in pore volume fraction and an increase in pore size from ~8 to ~25 nm in diameter (Fig. 5). There were other more subtle differences in coating microstructure. For coatings deposited at 900°C, SAD patterns from the coatings were roughly consistent with monazite, but diffraction spots were diffuse and streaked, and a fine (< 50 nm) grain size was inferred from the patterns. Diffraction contrast did not change abruptly across grains as the sample was tilted; instead, diffuse diffraction contrast swept irregularly across the coating, and identification of specific grains was difficult. Evidently the monazite coating grains were highly defective, but the defects could not be identified. For coatings deposited at 1300°C, diffraction patterns were sharp, with individual grains easily identifiable. Defects other than intragranular porosity were not observed. The coating grain size was often much greater than the coating thickness.

3.3.1. 1200°C heat-treatments

Coatings deposited at 900°C and then heat-treated at 1200°C had somewhat different microstructures. Two hours at 1200°C changed the defective, porous, and poorly crystallized monazite grains (Fig. 5) to small (40 nm diameter), well crystallized monazite grains with a small amount of porosity (Fig. 6). One hundred hours at 1200°C caused grain growth to ~100 nm diameter

with even less porosity. The most obvious features after 100 h at 1200°C were spheroidization of coatings less than 50 nm thick (Fig. 7), roughening of the monazite coating–fiber interface (Figs. 6–8), and facetting of alumina grains in the fiber and near the coating along basal planes (Figs. 6–8). Lanthanum segregation at facetted alumina–mullite interfaces near the coating was measured by analytical TEM (Fig. 8). Phosphorous segregation was not found, and lanthanum was not found in the interior of alumina grains. Wetting thin films were not observed along monazite–alumina, monazite–mullite, or alumina–mullite interphase boundaries, or along the corresponding triple junctions (Fig. 9).

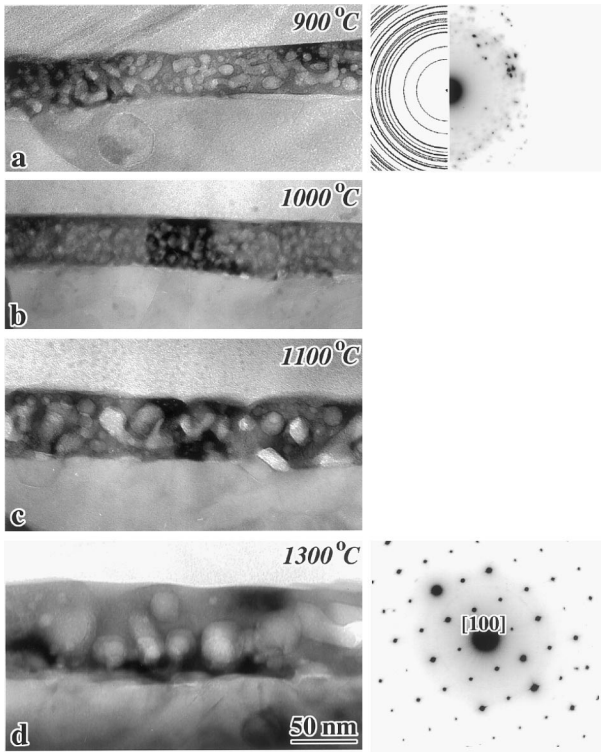

Fig. 5. TEM pictures of coating deposited at (a) 900°C, (b) 1000°C, (c) 1100°C, (d) 1300°C. Simulated and observed diffraction pattern of 900°C coating and observed diffraction pattern from a 1300°C coating are to the right.

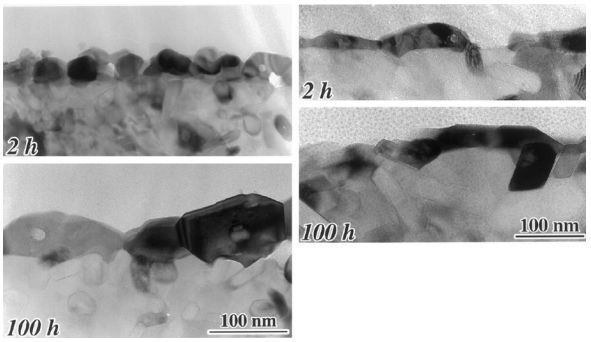

Fig. 6. TEM pictures of coating deposited at 900°C and later heat-treated at 1200°C for 2 h or 100 h.

3.4. Tensile strength

Coated filament tensile strength decreased from ~2 GPa[28] with both increased deposition temperature and with time at 1200°C after deposition at 900°C (Table 1, Fig. 10). Filaments coated at 1300°C had average tensile strengths of 1.21 GPa. Filaments heat-treated for 100 h at 1200°C after coating at 900°C had only 0.83 GPa average tensile strength. The actual average may have been slightly lower, because some filaments were too weak to mount in grips for tensile testing, and their contribution to the average would certainly have made it lower. Filaments coated at 1200°C were slightly stronger than those coated at 1100°C, as were filaments heat-treated for 2 h at 1200°C compared to 12 min at 1200°C. These observations were anomalous to the overall trend; it is possible that they are related to transient flaw healing, but more data is required to substantiate this.

Control experiments suggest that much of the strength drop may be unrelated to the presence of a coating. Filaments heat-treated for 100 h at 1200°C without a coating had only 1.04 GPa tensile strength (Table 1, Fig. 10). Similarly, filaments passed through the coating furnace at 1300°C and 1200°C had only ~1.5 GPa tensile strength, although filaments passed through water, water/HNO_3, ethanol, and water/1-octanol were stronger (Table 1, Fig. 10). The strength drop between fibers coated at 1000 and 1100°C was steeper than others, and may correlate with the slight

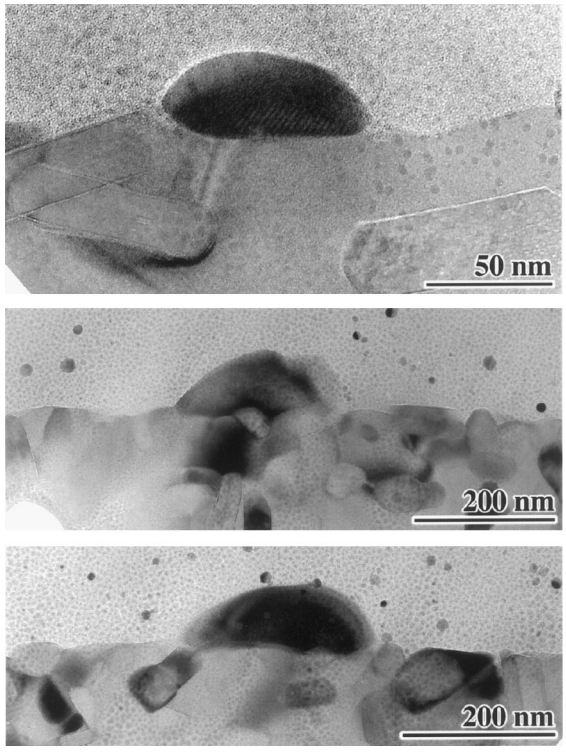

Fig. 7. TEM pictures of spheroidized coatings.

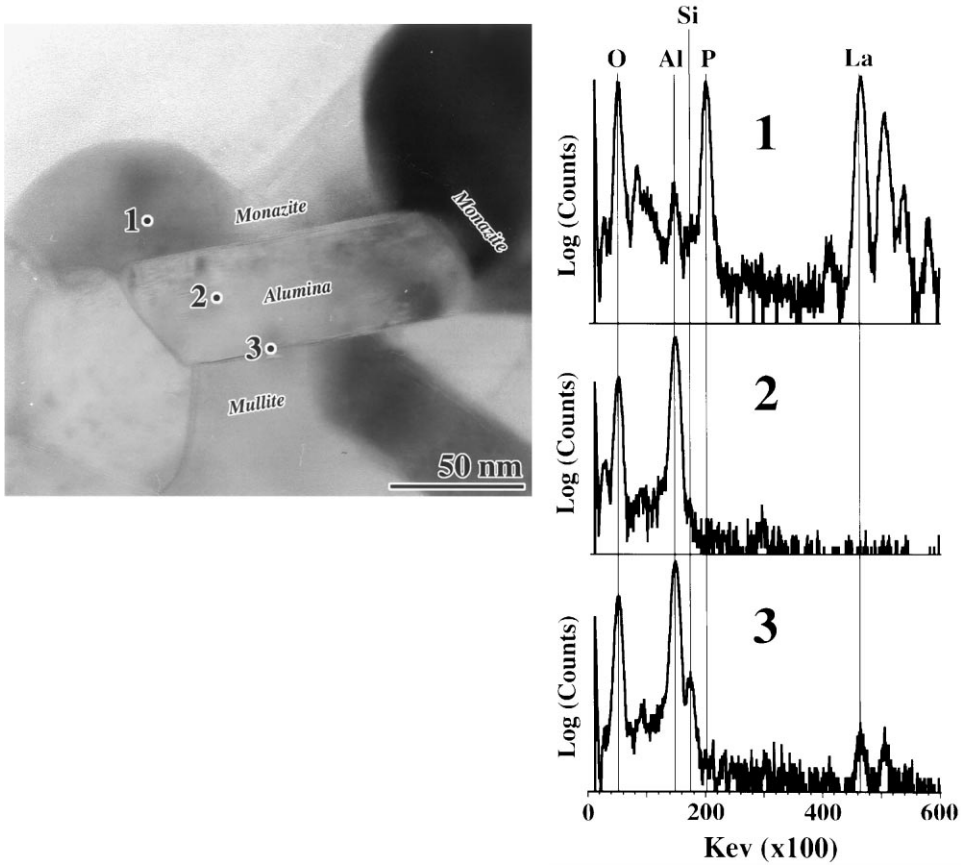

Fig. 8. TEM picture of an area around a monazite coating — fiber interface analyzed by TEM. The EDS spectra of spots 1, 2, and 3 on the image are shown to the right. Spot 3 at an alumina–mullite interphase boundary shows trace lanthanum.

increase in coating mass loss observed at about 950°C. Although the temperature interval does not exactly match, the heating rate was higher during coating than during the DTA/TGA measurements, so the corresponding mass loss during coating should be at a higher temperature. However, there are alternative explanations for this strength drop that will be discussed in the next section.

4. Discussion

Coating fibers with monazite at 900°C using this particular precursor preserves most of the original tensile strength. However, this would not eliminate tensile strength degradation if composites with these coated fibers were processed or used at or above 1200°C, as shown by tensile strengths of 900°C coated fiber heat-treated at 1200°C (Fig. 10). However, control experiments on uncoated fiber heat-treated at 1200°C have tensile strengths nearly as low as coated fibers. Beneath 1300°C grain growth is insignificant in Nextel 720.[38] The sensitivity of tensile strength to heat-treatment or coating atmosphere (Table 1) suggests that degradation is most

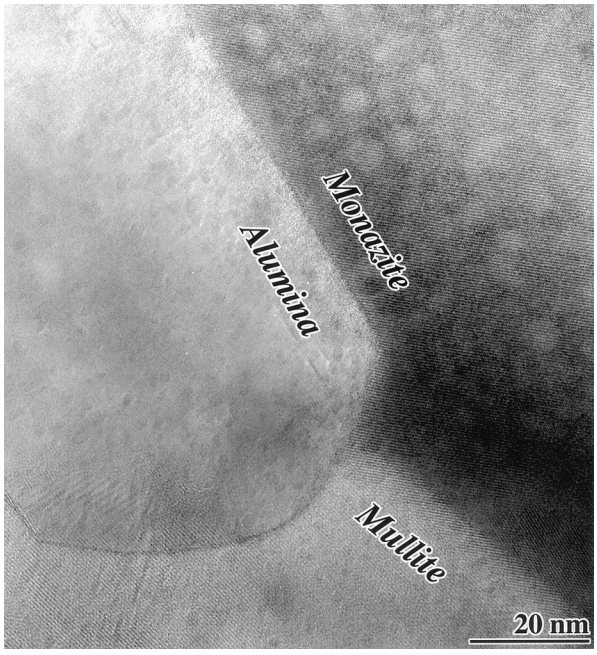

Fig. 9. High resolution TEM micrograph of a monazite–alumina–mullite triple junction at a coating–fiber interface. No evidence of a wetting phase at the interface or triple junction was found.

Table 1
Tensile strength measurements

No.	Deposition temperature (°C)	Coating	Environment	Heat-treatment temperature (°C)	Heat-treatment time (h)	Tensile strength (GPa)	Weibull modulus
1	900	Monazite	Air			1.95	6.85
2	1000	Monazite	Air			1.78	5.66
3	1100	Monazite	Air			1.32	4.95
4	1200	Monazite	Air			1.39	4.09
5	1300	Monazite	Air			1.21	5.09
5a	1300	Monazite	Argon			1.24	5.07
6	900	Monazite	Air	1200	0.02	1.14	3.77
7	900	Monazite	Air	1200	2	1.21	4.00
8	900	Monazite	Air	1200	100	0.83	3.43
9		Control	Air	1200	100	1.04	4.97
10	1200	Control	Air			1.50	4.79
11	1300	Control	Air			1.51	4.40
12	1300	Control	Water			1.77	4.23
13	1300	Control	Water/20% HNO_3			1.59	4.08
14	1300	Control	Water/20% HNO_3/l-octanol			1.85	5.11

likely environmental assisted surface crack growth. Previous work showed that coating thickness did not affect tensile strength, and that different monazite precursors used for fiber coating under identical conditions had much different tensile strengths, which was consistent with environmental effects specific to each precursor.[6] Flaws in weakly bonded fiber coatings should not function as fiber flaws,[19] which is consistent with lack of a coating thickness effect and the known debonding properties of monazite.

Observations made here and elsewhere[6] suggest that there are separate effects on fiber strength, one from the heat-treatment atmosphere, and one from the monazite precursor. It is not clear whether these effects are independent or synergistic. If degradation is predominantly environmental, hermetic matrices that seal fibers from the environment could preserve fiber strength in a CMC. For heat-treated fibers, atmospheric moisture or silica from $MoSi_2$ heating elements are possible corrosive chemical species.

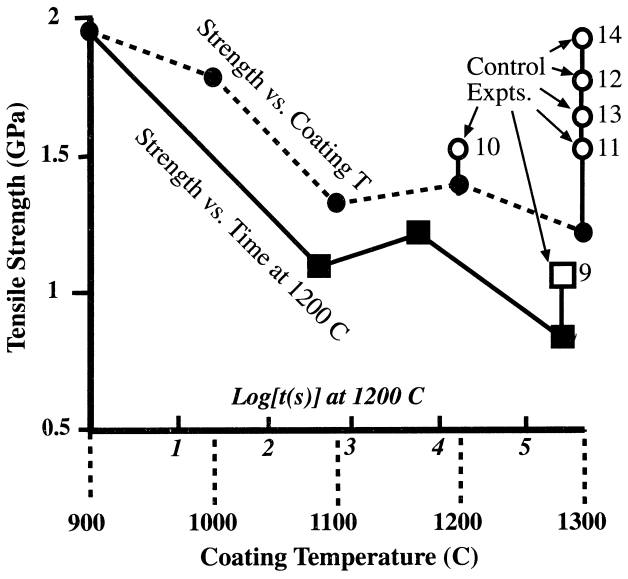

Fig. 10. Tensile strength of coated fibers and control experiments vs. coating temperature or heat-treatment time at 1200°C. Log(t) scale on x-axis refers to solid line connecting squares. Coating temperature scale on x-axis refers to dashed line connecting circles. Numbers for control experiments are given in Table 1.

At 1200°C segregation of lanthanum from monazite to interfaces in the fiber (Fig. 8) may also cause strength degradation. Lanthanum doped alumina has facetted and elongated grains.[39]

Lanthanum doping also retards sintering and creep in alumina.[39,40] Effects on strength have, to our knowledge, not been reported. If lanthanum segregation to alumina basal planes causes easier intergranular fracture along those planes analogous to cleavage in β-alumina and magnetoplumbites,[41,42] then significant weakening can be expected. We note that X-ray diffraction suggests our precursor was lanthanum rich (although TEM did not corroborate this). Therefore lanthanum activity may have been buffered to a relatively high value by La_3PO_7/$LaPO_4$, instead of a lower value fixed by $LaPO_4$/LaP_3O_9. More measurements of lanthanum segregation as a function of temperature, time, and lanthanum activity at the two different buffers needs to be measured, and a more definitive correlation with fiber tensile strength should be made.

Identification of the chemical species causing strength degradation remains problematic. Mass spectrometry suggests that only N_2 or CO, H_2O, and N_2O or CO_2 gases were evolved by the precursor above 700°C (Fig. 3). The black sample and argon atmosphere suggest that limited oxidation of carbon and partial reduction of the nitrates from the lanthanum precursor to N_2 and N_2O is more likely. The measured H_2O could also be an artifact

of wet tubing in the instrument, since background runs consistently found this gas despite attempts to run in a dry environment.[43] This leaves N_2 or N_2O as the most likely products of high temperature degassing, with H_2O, CO, CO_2, and undetected trace gases as additional possibilities. If H_2O or N_2 were the principal high temperature corrosive species, control experiments in air (72% nitrogen) and with water substituted for coating precursor could be expected to degrade fiber strength in a manner similar to the coated fibers. Unfortunately, this was not the case. Water "coated" fibers had some of the highest strengths of any control experiment (Fig. 10). Mass spectrometry of coating precursor was done in argon, but fiber coating was done in air, so the gases evolved during coating might be more highly oxidized forms of carbon and nitrogen than those found by mass spectrometry. However, fibers coated in argon with this precursor at 1300°C had 1.24 GPa tensile strength,[6] a negligible increase over those coated in air.

The partial pressure of the evolved gases is another concern. Partial pressures measured by mass spectrometry are quite low, because they are diluted by the argon atmosphere used for measurement. However, the partial pressure of a gas evolved in a closed coating pore may be much higher than atmospheric and depend on the bursting strength of the pore and the driving force for gas formation. If these gas filled pores are adjacent to the fiber surface, fiber surface flaws can be exposed to high pressure gas from precursor decomposition. As the pore volume fraction decreases with coating temperature (Fig. 5), it becomes more likely that the porosity is closed and that gas decomposition products are sealed in the coating. The large tensile strength drop between the 1000 and 1100°C coated fibers (Fig. 10) could, therefore, be related to densification and coarsening of coating porosity and the consequent transition from an open to a hermetic coating. However, if the main cause of strength degradation was environmental effects independent of the presence of a coating, such as those measured by control experiments, then it might also be argued that a hermetic coating should seal the fiber from this environment, and the fiber should be stronger. More information is necessary to confidently explain these results.

As deposited coatings were porous, particularly at low temperature, but the porosity formed during deposition at 900°C was not stable at 1200°C. These coatings recrystallized to a small grain size at 1200°C. Coatings deposited at 1300°C had a large grain size with somewhat larger intragranular porosity. Heat-treatments at 1200°C were not done on these 1300°C coated fibers. The large grain size and consequent lack of grain boundary diffusion pathways might cause this intragranular porosity to be more resistant to coarsening than the porosity present at 900°C. Further experiments are necessary to establish the T–t path dependence of coating microstructure.

The spheroidization of 50 nm thick coatings at 1200°C is another concern (Fig. 7). Previous analysis and observations of the Rayleigh instability of polycrystalline thin films suggests that monazite coatings on other oxides may be prone to this instability.[44,45] For example, the high monazite–alumina interphase boundary energy causes a large equilibrium contact angle θ between monazite and alumina, which in turn allows spheroidization of polycrystalline coatings at a smaller grain size (D) for a given coating thickness (a). Spheroidization is predicted when:[44]

$$\left(\frac{D}{a}\right) \geqslant \frac{3\sin^3\theta}{2-3\cos\theta+\cos^3\theta} \tag{1}$$

A more complex expression in later work[45] yields similar results. The grain size must be less than twice the coating thickness if the film is to be stable with respect to spheroidization at high θ. Coatings discussed in this paper (Figs. 5–7) had unusually large grain sizes in comparison to coatings made from other precursors,[6] so they may be particularly prone to spheroidization. Spheroidization kinetics of these coatings should depend on the surface diffusion coefficients of monazite.[46] However, when coated fibers are incorporated in a dense matrix, the rate determining process must change to interphase boundary diffusion control, which is generally slower than surface diffusion.[47] It is also necessary to transport either matrix or fiber material to accommodate monazite spheroidization, which could further retard spheroidization if diffusive mass transport in the fiber or matrix is slow compared to monazite.

5. Summary and conclusions

Lowering the deposition temperature of monazite from 1300 to 900°C for an ethanolic monazite precursor causes coatings from this particular precursor to have a higher pore volume fraction, smaller pore size, and defectively crystallized grains with poorly defined grain size. The porosity is mostly eliminated and the grains recrystallize during heat-treatment at 1200°C. Thin coatings spheroidized, which may be a problem with coatings like monazite that have high substrate interphase-boundary energy. Spheroidization kinetics may be retarded by incorporation of the coating in a dense matrix, and spheroidization can be prevented by stabilization of a small coating grain size in comparison to coating thickness.

Fibers coated at 900°C did not lose much tensile strength, but fibers coated at higher temperatures were more severely degraded. Control experiments that mimicked the deposition process in some cases were nearly as severely degraded as coated fibers. The high strengths of fibers coated at low temperatures was not

retained if those fibers were later heat-treated to higher temperatures. Again, degradation during heat-treatment was nearly as severe in control experiments without a coating.

Strength degradation at temperatures beneath 1200°C could not be caused by microstructural changes in the fiber because there is no grain growth at those temperatures. An environmental cause was suggested to be more likely. The chemical species in the environment or from coating degassing responsible for this degradation were not successfully isolated. It is also possible that strength degradation from the monazite coating was related to sealing of corrosive gas decomposition products in the coating at relatively high pressure and, therefore, related to transformation from open to closed porosity in the coating.

Lanthanum segregated from monazite to alumina-mullite interphase boundaries at 1200°C. Segregation was associated with roughening of the fiber-coating interface and facetting of alumina grains in the fiber. These microstructural changes may be at least partly responsible for low tensile strengths, but again it must be emphasized that these tensile strengths were not much lower than those for control experiments on uncoated fibers. More information on the kinetics and lanthanum activity dependence for segregation are desirable. It is clear that the tensile strength of Nextel 720, with or without coating, is sensitive to processing conditions, environment, and temperature. Further investigation of this sensitivity is necessary to optimize processing conditions for this fiber, and to design new fibers with improved properties.

Acknowledgements

We thank S. Sambasivan for the monazite precursor, D. Wilson of 3M for the Nextel 720 fiber, K. Von Lehmden for thin section preparation and tensile testing, J. Jones and P. Jero for mass spectrometry measurements, and K. Keller for manuscript review.

References

1. Mah, T., Mendiratta, M. G., Katz, A. P., Ruh, R. and Mazdiyasni, K. S., High-temperature mechanical behavior of fiber reinforced glass–ceramic–matrix composites. *J. Am. Cer. Soc.*, 1985, **68**(9), C248.
2. Naslain, R., Dugne, 0., Guette, A., Sevely, J., Brosse, C. R., Rocher, J. P. and Cotteret, J., Boron nitride interphase in ceramic matrix composites. *J. Am. Cer. Soc.*, 1991, **74**(101), 2482–2488.
3. Prewo, K. M., Brennan, J. J. and Starrett, S., Silicon carbide fiber-reinforced glass ceramic composite tensile behavior at elevated temperature. *J. Mat. Sci.*, 1989, **24**, 1373.
4. Zawada, L. P. and Wetherhold, R. C., The effects of thermal fatigue on a SIC fiber/aluminosilicate glass composite. *J. Mat. Sci.*, 1991, **26**, 648–654.
5. Sun, E. Y., Lin, H.-T. and Brennan, J. J., Intermediate-temperature environmental effects on boron nitride-coated silicon carbide-fiber-reinforced glass–ceramic composites. *J. Am. Ceram. Soc.*, 1997, **80**(31), 609–614.
6. Boakye, E., Hay, R. S. and Petry, M. D. Continuous coating of oxide fiber tows using liquid precursors: monazite coatings on Nextel 720. *J. Am. Ceram. Soc.*, 1999, **82**(9), 2321–2331.
7. Morgan, P. E. D. and Marshall, D. B., Functional interfaces for oxide/oxide composites. *Mat. Sci. Eng.*, 1993, **A162**, 15–25.
8. Morgan, P. E. D. and Marshall, D. B., Ceramic composites of monazite and alumina. *J. Am. Cer. Soc.*, 1995, **78**(61), 1553–1563.
9. Morgan, P. E. D., Marshall, D. B. and Housley, R. M., High temperature stability of monazite–alumina composites. *J. Mat. Sci. Eng.*, 1995, **A195**, 215–222.
10. Kanazawa, C., Johnson, S. M. and Porter, J. R., Monazite coating promotes fiber pullout. *J. Am. Ceram. Soc.*, 1997, **80**(7), Back Cover.
11. Kuo, D.-H. and Kriven, W. M., Characterization of yttrium phosphate and a yttrium phosphate/yttrium aluminate laminate. *J. Am. Ceram. Soc.*, 1995, **78**(111), 3121–3124.
12. Goettler, R. W., Sambasivan, S. and Dravid, V. P., Isotropic complex oxides as fiber coatings for oxide–oxide CFCC. *Ceram. Eng. Sci. Proc.*, 1977, **18**(3), 279–286.
13. Davis, J. B., Marshall, D. B., Housley, R. M. and Morgan, P. E. D., Machinable ceramics containing rare-earth phosphates. *J. Am. Ceram. Soc.*, 1998, **81**(8), 2169–2175.
14. Hay, R. S., Davis, J. B., Marshall, D. B. and Morgan, P. E. D., Presented at the 1998 Annual Meeting of the Am. Ceram. Soc.
15. Hwang, T. J., Hendrick, M. R., Shao, H., Hornis, H. G. and Hunt, A. T., Combustion chemical vapor deposition (CCVD) of $LaPO_4$ monazite and beta-alumina on alumina fibers for ceramic matrix composites. *Mater. Sci. Eng. A*, 1998, **244**, 91–96.
16. Chayka, P, personal communication.
17. Hay, R. S., Petry, M. D. and Boakye, E. Fiber strength with coatings from sols and solutions. Presented at the 20th Annual Conference on Composites and Advanced Ceramics, Cocoa Beach, 1996.
18. Helmer, T., Peterlik, H. and Kromp, K., Coating of carbon fibers — the strength of the fibers. *J. Am. Ceram. Soc.*, 1995, **78**(1), 133–136.
19. Parthasarathy, T. A., Folsom, C. A. and Zawada, L. P., Combined effects of exposure to salt (NaCI) water and oxidation on the strength of uncoated and BN-coated nicalon fibers. *J. Am. Ceram. Soc.*, 1998, **81**(7), 1812–1818.
20. Trumbauer, E. R., Hellmann, J. R., Shelleman, D. L. and Koss, D. A., Effect of cleaning and abrasion induced damage on the Weibull strength distribution of sapphire fiber. *J. Am. Cer. Soc.*, 1994, **77**(8), 2017–2024.
21. Inniss, D., Zhong, Q. and Kurkjian, C. R., Chemically corroded pristine silica fibers: blunt or sharp flaws. *J. Am. Ceram. Soc.*, 1993, **76**(12), 3173–3177.
22. Chang, X. and Du, Y., Electrolytic treatment of continuous CVD silicon carbide fibers. *J. Am. Ceram. Soc.*, 1997, **80**(10), 2754–2756.
23. Fernando, J. A., Chawla, K. K., Ferber, M. K. and Coffey, D., Effect of boron nitride coating on the tensile strength of Nextel 480 fiber. *Mater. Sci. Eng. A*, 1992, **154**, 103–108.
24. Curtin, W. A., Strength versus gauge length in ceramic–matrix composites. *J. Am. Cer. Soc.*, 1994, **77**(4), 1072–1074.
25. Curtin, W. A., In situ fiber strengths in ceramic–matrix composites from fracture mirrors. *J. Am. Ceram. Soc.*, 1994, **77**(4), 1075–1078.
26. Curtin, W. A., Ahn, B. K. and Takeda, N., Modeling brittle and tough stress-strain behavior in unidirectional ceramic matrix composites. *Acta Mater.*, 1998, **46**(10), 3409–3420.
27. Jones, J. G., Busbee, J. D., Jero, P. D., Kent, D. J. and Liptak, D. C. In situ control of interface coatings on fibers using CVD. In: *Composites and Functionally Graded Materials*, ed. Srivatsan, T. S. et al., ASME, Vol. **80**, 1997, pp. 379–384

28. Wilson, D. M., Statistical tensile strength of Nextel 610 and Nextel 720 fibres. *J. Mat. Sci.*, 1997, **32**, 2535–2542.
29. Wilson, D. M., Lieder, S. L. and Lueneburg, D. C., Microstructure and high temperature properties of Nextel 720 fibers. *Cer. Eng. Sci. Proc.*, 1995, **16**(5), 1005–1014.
30. Anon. *3M Nextel Textiles Product Description Brochure* 3M, St. Paul, MN
31. Hay, R. S. Method for coating continuous tows. US Patent 5, 164,229, 1993.
32. Hay, R. S. and Hermes, E. E. Coating apparatus for continuous fibers. US Patent 5,217,533, 1993.
33. Hay, R. S., Sol–gel coating of fiber tows. *Cer. Eng. Sci. Proc.*, 1991, **12**(7–8), 1064.
34. Hay, R. S. and Hermes, E. E., Sol–gel coatings on continuous ceramic fibers. *Cer. Eng. Sci. Proc.*, 1990, **11**(9–10), 1526–1532.
35. Cinibulk, M. K., Welch, J. R. and Hay, R. S., Preparation of thin sections of coated fibers for characterization by transmission electron microscopy. *J. Am. Ceram. Soc.*, 1996, **79**(9), 2481–2484.
36. Hay, R. S., Welch, J. R. and Cinibulk, M. K., TEM specimen preparation and characterization of ceramic coatings on fiber tows. *Thin Solid Films*, 1997, **308–309**, 389–392.
37. Petry, M. D., Mah, T. and Kerans, R. J., Validity of using average diameter for determination of tensile strength and Weibull modulus of ceramic filaments. *J. Am. Ceram. Soc.*, 1997, **80**(10), 2741–2744.
38. Welch, J. R. and Hay, R. S. Presented at the Annual Meeting of the American Ceramic Society, 1997.
39. Cho, J., Harmer, M. P., Chan, H. M., Rickman, J. M. and Thompson, A. M., Effect of yttrium and lanthanum on the tensile creep behavior of aluminum oxide. *J. Am. Ceram. Soc.*, 1997, **80**(4), 1013–1017.
40. Fang, J., Thompson, A. M., Harmer, M. P. and Chan, H. M., Effect of yttrium and lanthanum on the final-stage sintering behavior of ultrahigh-purity alumina. *J. Am. Ceram. Soc.*, 1997, **80**(8), 2005–2012.
41. Phillips, W. R. and Griffen, D. T., *Optical Mineralogy — The Non-Opaque Minerals*. W. H. Freeman & Co, San Francisco, 1981, p. 677.
42. Cinibulk, M. K. and Hay, R. S., Textured magnetoplumbite fiber-matrix interphase derived from sol–gel fiber coatings. *J. Am. Ceram. Soc.*, 1996, **79**(5), 1233–1246.
43. Jones, J. G. personal communication, 1998.
44. Srolovitz, D. J. and Safran, S. A., Capillary instabilities in thin films. I. Energetics. *J. Appl. Phys.*, 1986, **60**(1), 247–254.
45. Miller, K. T., Lange, F. F. and Marshall, D. B., The instability of polycrystalline thin films: experiment and theory. *J. Mater. Res.*, 1990, **5**(11), 151–160.
46. Srolovitz, D. J. and Safran, S. A., Capillary instabilities in thin films. II. Kinetics. *J. Appl. Phys.*, 1986, **60**(1), 255–260 .
47. Dynys, J. M., Coble, R. L., Coblenz, W. S. and Cannon, R. M., Mechanisms of atom transport during initial stage sintering of Al_2O_3. In *Sintering Processes*, ed. G. C. Kuczynski. Metals Park, OH, American Society for Metals/Plenum Press, 1980, pp. 391.